

Induced burst of fluid drops in a two-component lattice Bhatnager-Gross-Krook fluid

I. Halliday and C. M. Care

Division of Applied Physics and Materials Research Institute, Sheffield Hallam University, Pond Street, Sheffield S1 1WB, United Kingdom

S. Thompson and D. White

Materials Research Institute, Sheffield Hallam University, Pond Street, Sheffield S1 1WB, United Kingdom

(Received 20 February 1996)

We describe a two-dimensional simulation of burst in neutrally buoyant drops subject to shear using a two-component, two-speed lattice Bhatnager-Gross-Krook (BGK) fluid. Measuring the dependence of critical shear rate for drop rupture on flow parameters, our results validate the method over a range of simulation variables. The model's interfacial tension parameter σ , undeformed drop radius, and BGK relaxation parameter ω are all found to have the correct influence upon the process of burst required by simple hydrodynamic theory. Within the model, the macroscopic surface tension and fluid viscosity are coupled; however, this does not limit the application of the technique. [S1063-651X(96)11008-4]

PACS number(s): 47.55.Dz, 05.50.+q

The mechanical formation of emulsions from multicomponent immiscible fluid mixtures is a complex problem of considerable technological and theoretical interest. Advection of suspended drops and marked departures in shape before burst reduce the utility of traditional numerical methods. However, competitor lattice Boltzmann (LB) techniques allow the simulator to calculate the flow of a viscous incompressible fluid by solving the dynamics of colliding and propagating prototype particles on a regular lattice using a Boltzmann type equation [1]. The simplest and probably most tractable lattice Boltzmann variant derives its inspiration from the work of Bhatnagar, Gross, and Krook on the Boltzmann equation of statistical physics [2]. The appropriately named lattice BGK method [3–5], then, incorporates both isotropy and Galilean invariance directly into a model that has the advantage of simple collision step and that has been shown to recover single phase hydrodynamics [3–5].

Two-dimensional lattice Boltzmann *immiscible* lattice gas (LBILG) techniques [6] have been applied to droplets under shear to demonstrate qualitatively correct steady-state interfacial hydrodynamic boundary conditions [7] and, in three dimensions, to sheared phase separation [8]. The growing literature on this method has been recently reviewed by Rothmann and Zaleski [9].

Here we report on simulations using a LBILG BGK algorithm enhanced to contain different species and an interface, with advantages similar to the model in [7], applying the method to the simulation of burst in an infinite, equispaced line of neutrally buoyant *red* fluid component drops suspended along the x axis, within a *blue* component, the flow in the far field of which is a uniform shear of rate $\dot{\gamma}$ [10].

As we have commented, an attractive feature of the BGK approach is its simple collision step with a scalar collision operator ω controlling the simulated fluid kinematic viscosity through [4]

$$\nu = \frac{1}{6} \left[\frac{2}{\omega} - 1 \right]. \quad (1)$$

Designated D2Q9 [4], our lattice BGK algorithm uses a square lattice with links \mathbf{c}_i to both nearest and next-nearest neighbors. As such we use a two-speed lattice, the multi-speed nature of which requires careful consideration when incorporating algorithmic extensions designed to separate red and blue densities $R_i(\mathbf{x}, t)$, $B_i(\mathbf{x}, t)$ [6]. As a measure of local gradient in the color distribution, a local “color field” $\mathbf{f}(\mathbf{x}, t)$ is calculated using direction-weighted contributions of chromatic link densities from $\mathbf{f}(\mathbf{x}, t) = \sum_{ij} [R_j(\mathbf{x} + \mathbf{c}_i, t) - B_j(\mathbf{x} + \mathbf{c}_i, t)] \mathbf{c}_i$ [6,7]. The BGK collision step redistributes achromatic density $N_i(\mathbf{x}, t) \equiv R_i(\mathbf{x}, t) + B_i(\mathbf{x}, t)$ to links according to the local flow conditions. The tendency of an equivalent automaton color segregation algorithm [11] to accumulate (denude) density on links perpendicular (parallel) to an interface line is introduced at this stage, after Gunstensen *et al.* [6], by applying perturbations to link densities with reference to the direction of $\mathbf{f}(\mathbf{x}, t)$, the amplitude of these perturbations having a linear dependence on a “surface tension” parameter σ [7]. However, it should be noted that Gunstensen *et al.* use a linearized lattice Boltzmann scheme rather than the BGK method described in this work. Color is allocated to collided, perturbed link densities in that distribution which maximizes the work done by a color flux in the direction of the color field [6,7]. Essentially, all that is necessary to achieve such an allocation is that as much red (blue) as possible should color the density on the link \mathbf{c}_i of largest (smallest) projection onto the direction of $\mathbf{f}(\mathbf{x}, t)$.

For a surface tension algorithm such as ours, it may be shown [10,11] that the form of the macroscopic surface tension Σ takes the form

$$\Sigma(\sigma, \omega) \sim \sigma/\omega, \quad (2)$$

where ω determines lattice fluid kinematic viscosity as given in Eq. (1). Other LBILG's exhibit similar dependence of Σ upon collision parameters and hence viscosity. In [6], Σ is shown to depend directly upon λ^{-1} where λ is that eigenvalue of the collision matrix which determines the simulated fluid kinematic viscosity through $\nu = -\frac{1}{8}(2\lambda^{-1} + 1)$. The de-

pendence of Σ upon a collision parameter in an LB fluid has important consequences to which we shall return.

Having initialized links within a circular central portion of lattice with red density to form a drop, a shear in the x direction was applied in its far field to the outlying blue fluid by perturbing appropriate lattice-edge link densities [7]. The observed shear rate $\dot{\gamma}$ generated by this perturbation was measured as the mean value of $\partial v_x / \partial y$ over a horizontal layer 6 sites deep, always centered a fixed vertical distance from the axis of the line of undeformed drops. A position for this layer, sufficiently far from the axis to render the measured shear rate sensibly independent of system and drop size, was easy to establish for $\dot{\gamma}$ was observed to be constant over much of the blue fluid.

For the large distortions encountered in this work, approximate theories cease to apply and we here characterize drop shape and orientation only in terms of a , the largest distance from the center of mass O to any point A on the perimeter (defined by mixed color sites) and drop orientation α , the angle subtended at the horizontal by \vec{OA} .

All results derive from steady-state drops with undeformed radii R : $10 < R < 20$ lattice spacings, each evolved (collided, streamed) for 20 000 lattice updates, over which site density was initialized to 1.8 and unless otherwise stated, results relate to lattices of 90×60 . Sizes of up to 140×93 were used to minimize size effects and to facilitate comparisons between drops of different initial radii, when overall lattice proportions were scaled with the initial radius. The range of surface tension parameter σ was determined by requiring the interfacial density perturbations be less than 10% of a typical nonzero velocity link density. The range of parameter ω was determined from considerations of equilibration time and stability [4].

Figure 1 illustrates a progressive drop distortion with increasing applied shear, the constant direction of which is indicated by the arrows in frame 1(a). The sequence demonstrates progressively greater departure from an initially ellipsoidal shape well before a critical shear rate $\dot{\gamma}_c$ is reached, where rupture into two or more drops occurs depending on conditions. $\dot{\gamma}_c$ was measured by increasing the perturbations applied to lattice-edge densities (throughout, these remained $< 10\%$ of unforced values), allowing stabilization and measuring the resulting blue fluid shear rate while observing the final configuration of the drop(s). In this way one can determine, to any required accuracy, the value of $\dot{\gamma}$ at which rupture occurs, and its associated error, by extrapolating the (linear) graph of applied $\dot{\gamma}$ against lattice-edge perturbation beyond the last observed $\dot{\gamma}$ admitting of a whole drop. Note that $\dot{\gamma}_c$ was obtained, as for all data, at a fixed distance from the drop, in a horizontal layer of sites 25 lattice units off center.

According to approximate theory [7,12] the drop orientation α increases linearly in small applied shear. In a typical variation between α and $\dot{\gamma}$, Fig. 2 shows this linear regime in our data when $\dot{\gamma}$ is well away from the critical value. It is tempting to associate the point at which a curve of the form $\alpha = A(\dot{\gamma} - \dot{\gamma}_c)^K$ fitted through these data cuts the abscissa with the critical shear rate $\dot{\gamma}_c$ and, within the limits of observational accuracy, this did appear to be the case. However,

the latter quantity, as recorded in Figs. 3–5, was actually determined as discussed above.

Taylor [13] first approximated, in the surface tension (small deformation) regime, a maximum stable radius R for drops suspended in shear fields, which may withstand the disruptive viscous stresses of the shearing fluid,

$$R = \frac{8\Sigma(\eta + \eta')}{\dot{\gamma}_c(19\eta' + 16\eta)}, \quad (3)$$

with η (η') the suspending (drop) fluid shear viscosity. In our results (e.g., Fig. 1) even drops with large surface tensions depart markedly from a spherical form before burst. Strictly, Taylor's estimate (3) only indicates the conditions under which marked deviations from a spherical shape occur. However, when one considers that the only adimensional quantities that can be constructed with the parameters of the problem are a capillary number $\Sigma/R\eta\dot{\gamma}_c$ and viscosity ratio $\phi = \eta/\eta'$ it becomes clear that, at least, the general form of the last equation is valid as a means for predicting $\dot{\gamma}_c$ in terms of the present flow's parameters. Equation (3) is therefore taken as a basis for comparison with theory and by rearranging it we obtain a functional form for the critical shear rate $\dot{\gamma}_c$ at a rupture of

$$\dot{\gamma}_c = \frac{\Sigma}{R\eta} f(\phi), \quad (4)$$

where f is a function of only ϕ and which, on the basis of Taylor's approximation [Eq. (3)], would be of the form $f(\phi) = (a + b\phi)/(c + d\phi)$. We assume that (4) applies to our model and, substituting from (1) and (2), we take the dependence of $\dot{\gamma}_c$ upon simulation parameters ω , ϕ , and σ for this lattice BGK fluid to be of the form

$$\dot{\gamma}_c \sim \frac{\sigma}{R} g(\rho, \phi) \left(\frac{1}{2 - \omega} \right), \quad (5)$$

where ρ denotes lattice density and $g(\rho, \phi)$ may be related to $f(\phi)$ by using (4) and the relation $v = \eta/\rho$. The need for a specific determination of the function $g(\rho, \phi)$ may be avoided by restricting the BGK parameter ω to take the same value in both fluids and hence $\phi = 1$ in all our results.

Figures 3 and 4 exhibit the proportional dependence of $\dot{\gamma}_c$ upon independent parameter σ and $1/R$ as predicted by (5), for simulations in which the BGK relaxation parameter for both fluids is held fixed at $\omega = 0.91$. For Fig. 3, the undeformed drop radius was maintained constant at $R = 13$. In the case of Fig. 4 the surface tension parameter was fixed at $\sigma = 0.0075$, and the lattice size was scaled to maintain a constant proportion between drop radius R and the linear lattice dimension.

Figure 5 shows the variation in $1/\dot{\gamma}_c$ with the BGK relaxation parameter ω for fixed interfacial perturbation parameter $\sigma = 0.0075$ and undeformed radius $R = 13$. $\dot{\gamma}_c$ was obtained for a range of equal red and blue fluid BGK relaxation parameters $0.7 \leq \omega \leq 1.4$, thereby maintaining the viscosity ratio ϕ constant. Collision parameter ω influences the model's macroscopic surface tension through (2) and hence (5). This latter equation predicts a linear dependence of $1/\dot{\gamma}_c$ upon ω , other parameters being constant, and Fig. 5 provides sup-

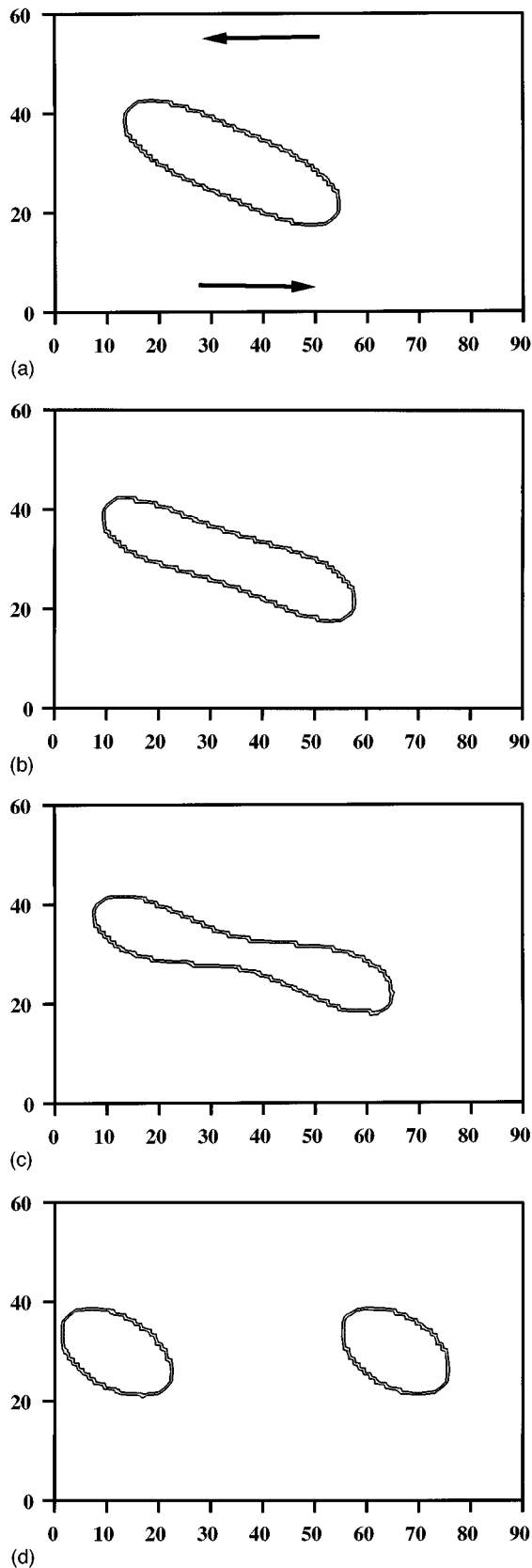


FIG. 1. Contour plots of constant red density depict a selection of four configurations [(a)–(d)] in the progressive deformation and eventual burst of a drop of original radius $R=13$ lattice spacings in applied shear fields of 3.270×10^{-3} , 3.503×10^{-3} , 3.569×10^{-3} , and 3.500×10^{-3} (time steps) $^{-1}$, on a lattice of 90×60 . The BGK relaxation parameter in use for these data was $\omega=0.91$ and the interfacial tension perturbation parameter was $\sigma=0.0075$.

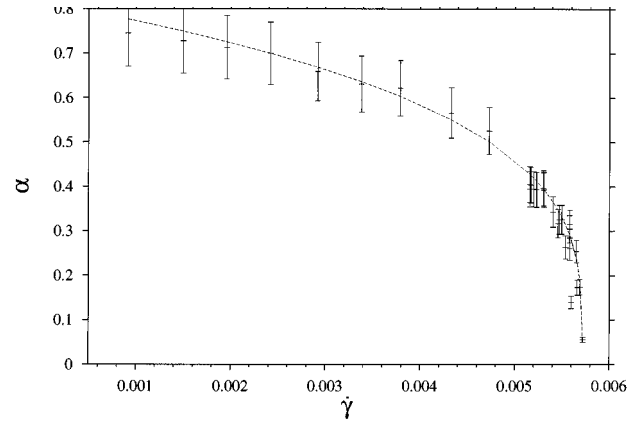


FIG. 2. A typical variation of α with $\dot{\gamma}$ for a drop with undeformed radius $R=13$. $\omega=0.91$ for both fluids and $\sigma=0.0075$ on a lattice of xy dimension of 90×60 . The line fitted through this data is $\alpha=A(\dot{\gamma}-\dot{\gamma}_c)^K$. Optimum fit is obtained with the parameters $A=3.2$, $K=0.27$, $\dot{\gamma}_c=0.0057$.

port for this prediction. The recorded values of $1/\dot{\gamma}_c$ lie approximately on a line of best fit with gradient to intercept with a ratio of -0.41 against the predicted ratio -0.5 and this perhaps suggests that the model may need to be analyzed in terms of an effective relaxation parameter, possibly of the form $\omega' = k\omega$. Caution needs to be exercised, however, bearing in mind the excellent agreement with the simulation of Eq. (1) [4] and also the effect of such a modification upon macroscopic surface tension, through (2).

It is known [12] that high viscosity drops may be broken (after long times) by solenoidal (irrotational) flows but are invulnerable to flows with high vorticity. The range of our simulated fluids' kinematic viscosities was restricted and for larger values of the latter parameter ($\nu > 1$, corresponding to $\omega < 0.29$) the drop did not rupture with the simulationally accessible applied (nonsolenoidal) shears, instead appearing to align indefinitely to the horizontal.

In conclusion, using a lattice Boltzmann fluid we have simulated rupture in neutrally buoyant, immiscible fluid

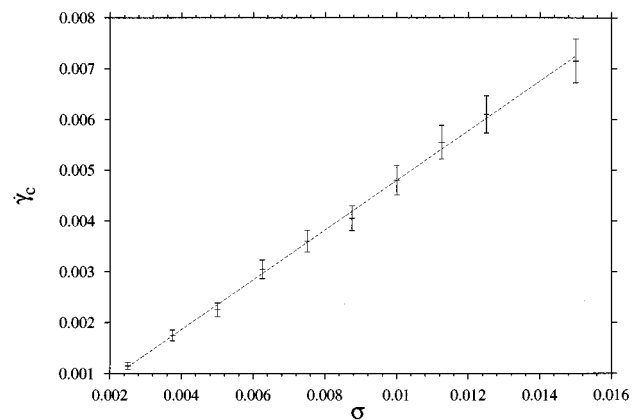


FIG. 3. Variation in $\dot{\gamma}_c$, with interface perturbation parameter σ in the range $0.002 \leq \sigma \leq 0.016$ with $\omega=0.9$ in both fluids. All data were obtained from a drop of constant undeformed radius R of 13 lattice units on a lattice of xy dimension 90×60 . The solid line represents a straight-line least squares fit with an ordinal intercept of 9.5×10^{-5} .

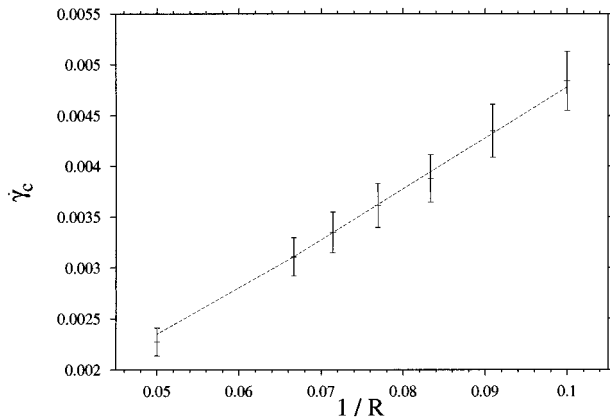


FIG. 4. Dependence of $\dot{\gamma}_c$ on reciprocal drop radius R with $10 \leq R \leq 20$ (lattices 76×56 – 140×92) for a drop with fixed surface tension parameter $\sigma = 0.0075$, and $\omega = 0.91$ in both fluids. The solid line represents the least squares fit to the data with an ordinal intercept of -2.3×10^{-4} (time steps) $^{-1}$.

drops of various undeformed radii R , surface tension σ , and BGK relaxation ω parameters. The dependence of macroscopic surface tension Σ upon σ and ω does not impinge upon useful application of the method since a simulator may fix ν , ϕ (via ω , ω'), and thereafter adjust Σ through σ . However, the data of Fig. 5 suggest a possible need to refine our present understanding of the interplay between σ and BGK relaxation parameter ω beyond first order in velocity.

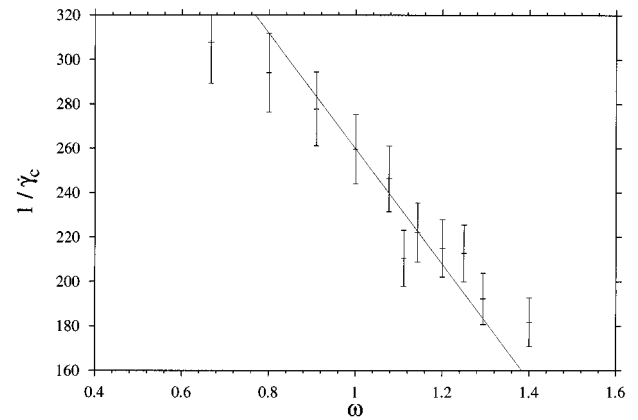


FIG. 5. Dependence of reciprocal $\dot{\gamma}_c$ on BGK parameter ω ($0.7 \leq \omega \leq 1.4$), for drops with constant surface tension perturbation parameter $\sigma = 0.0075$ and undeformed radius $R = 13$ lattice units. The solid line represents a least squares fit to these data obtained by varying the ordinal intercept c in such a way as to maintain the ratio $m/c = -0.5$, where m is the gradient.

The dependence of measured critical shear rate $\dot{\gamma}_c$ for drop burst upon all independent simulation parameters is, overall, in good agreement with a simple hydrodynamic theory and the established relationships between, for example, ω and ν [4]. The method should apply in any regime and capture the hydrodynamic interactions of drops formed *after* rupture, which provides for useful applications.

-
- [1] U. Frisch, D. d’Humières, B. Hasslacher, P. Lallemand, Y. Pomeau, and J. P. Rivet, *Complex Syst.* **1**, 649 (1987), and references therein.
- [2] P. Bhatnagar, E. P. Gross, and M. K. Krook, *Phys. Rev.* **94**, 511 (1954).
- [3] R. Kingdon (private communication).
- [4] Y. H. Qian, D. d’Humières, and P. Lallemand, *Europhys. Lett.* **17**, 479 (1992).
- [5] H. Chen, S. Chen, and W. H. Matthaeus, *Phys. Rev. A* **45**, 5339 (1992).
- [6] A. K. Gunstensen, D. H. Rothman, S. Zaleski, and G. Zanetti, *Phys. Rev. A* **43**, 4320 (1991).
- [7] I. Halliday and C. M. Care, *Phys. Rev. E* **53**, 1602 (1996).
- [8] J. Olson and D. Rothman, *J. Stat. Phys.* **81**, 199 (1995).
- [9] D. Rothman and S. Zaleski, *Rev. Mod. Phys.* **66**, 1417 (1994).
- [10] I. Halliday and C. M. Care (unpublished).
- [11] D. H. Rothman and J. M. Keller, *J. Stat. Phys.* **52**, 1119 (1988).
- [12] J. M. Rallison, *Annu. Rev. Fluid. Mech.* **16**, 45 (1984).
- [13] G. I. Taylor, *Proc. R. Soc. London Ser. A* **138**, 41 (1932).